ACS APPLIED MATERIALS & INTERFACES

Letter

www.acsami.org

Layered Bi_2Se_3 Nanoplate/Polyvinylidene Fluoride Composite Based n-type Thermoelectric Fabrics

Chaochao Dun,[†] Corey A. Hewitt,[†] Huihui Huang,*[,†,‡] Junwei Xu,[†] David S. Montgomery,[†] Wanyi Nie,[§] Qike Jiang,[∥] and David L. Carroll*[,†]

[†]Center for Nanotechnology and Molecular Materials, Department of Physics, Wake Forest University, Winston-Salem, North Carolina 27109, United States

[‡]SZU-NUS Collaborative Innovation Center for Optoelectronic Science & Technology, Key Laboratory of Optoelectronic Devices and Systems of Ministry of Education and Guangdong Province, College of Optoelectronic Engineering, Shenzhen University, Shenzhen 518060, China

[§]Chemistry Division, Los Alamos National Laboratory, Los Alamos, New Mexico 87544, United States

[∥]Dalian Institute of Chemical Physics, Chinese Academy of Sciences, Dalian 116023, China

Supporting Information

ABSTRACT: In this study, we report the fabrication of n-type flexible thermoelectric fabrics using layered Bi_2Se_3 nanoplate/polyvinylidene fluoride (PVDF) composites as the thermoelectric material. These composites exhibit room temperature Seebeck coefficient and electrical conductivity values of -80 μV K^{-1} and 5100 S m^{-1}, respectively, resulting in a power factor approaching 30 μW m^{-1}K^{-2}. The temperature-dependent thermoelectric properties reveal that the composites exhibit metallic-like electrical conductivity, whereas the thermoelectric power is characterized by a heterogeneous model. These composites have the potential to be used in atypical applications for thermoelectrics, where lightweight and flexible materials would be beneficial. Indeed, bending tests revealed excellent durability of the thermoelectric fabrics. We anticipate that this work may guide the way for fabricating high performance thermoelectric fabrics based on layered V−VI nanoplates.

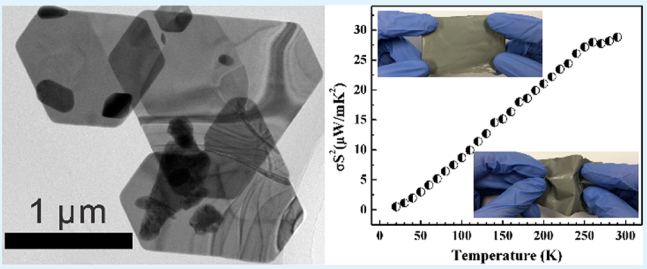

KEYWORDS: *thermoelectric, layered materials, flexible, bismuth selenide, topological insulator*

1. INTRODUCTION

The growing market of portable/wearable electronic devices has stimulated research interests in flexible, renewable, and sustainable energy sources, including solar, thermoelectric, and piezoelectric.[1−4] Among them, flexible thermoelectric generators have attracted tremendous attention because of their potential for integratation into portable/wearable electronic devices attributable to their ability to directly generate electricity from waste heat such as that from the human body.[1,5] Recently, much research has focused on studying flexible thermoelectric-based materials, including conductive polymers[6,7] and inorganic/organic composites.[8,9] For example, researchers have reported that doped poly(3,4-ethylenedioxythiophene) (PEDOT) thin films possess a high room temperature figure of merit value over 0.2.[6,10] Additionally, previous reports have found that it is possible to improve the thermoelectric performance of conductive polymer-based thin films by adding inorganic nanomaterials, such as carbon nanotubes[11−13] and Bi_2Te_3 nanowires.[14] However, most conductive polymer-based materials are p-type semiconductors that only generate positive thermoelectric power. Therefore, the development of high performance, flexible n-type thermoelectrics with negative thermoelectric power is necessary for fabricating thermoelectric generators with multiple element modules.[1] The thermoelectric composites based on n-type inorganic nanomaterials and nonconducting polymers possess the advantage of using cheap nonconducting polymers with ultralow thermal conductivity, such as polyvinylidene fluoride (PVDF), instead of expensive conductive polymers.[1,15]

As mentioned above, the efficiency of a thermoelectric material is usually evaluated by a dimensionless thermoelectric figure of merit $ZT = \alpha^2\sigma T/\kappa$, where α, σ, T, and κ are the Seebeck coefficient, electrical conductivity, absolute temperature, and thermal conductivity, respectively. Therefore, to develop high performance thermoelectric materials, it is essential to decouple these thermoelectric parameters even though they are usually interdependent according to the Wiedemann−Franz law.[16] Recent studies have found that the ZT value could be enhanced through nanostructuring of thermoelectric materials by decreasing κ with little change to the other thermoelectric properties,[17−20] which is one promising method for fabricating high performance thermoelectrics. Among all thermoelectric

Received: January 19, 2015
Accepted: March 23, 2015
Published: March 23, 2015

DOI: 10.1021/acsami.5b00514
ACS Appl. Mater. Interfaces 2015, 7, 7054−7059

materials, V_2VI_3-type compounds (especially Bi_2Se_3, Bi_2Te_3, and Sb_2Te_3) are the best-known bulk thermoelectric materials that exhibit high ZT values.[17,21] Recent developments have renewed the interest in V_2VI_3-type compounds that show insulating properties in the bulk phase but robust metal-like surface states derived from the combination of spin−orbit interactions and time-reversal symmetry, namely, topological insulators.[22,23] Furthermore, V_2VI_3-type compounds possess stacked layers of a laminated structure that are weakly bonded by van der Waals forces. Each layer is one quintuple layer (QL), and the five atoms are covalently bonded together along the z axis in the order of VI-V-VI-V-VI. Therefore, the layered structures allow V_2VI_3 to be easily fabricated as two-dimensional (2D) nanoplates with atomic thicknesses.[24] Also, the novel surface properties of the topological insulators could be greatly enhanced in the 2D structure due to the ultralarge surface-to-volume ratio. It was previously reported that by virtue of these properties, the thermoelectric performances of these materials could be strongly enhanced in their 2D structure.[9,18,19,25,26]

Here, we explore the idea of fabricating flexible thermoelectric generators based on heterogeneous thin films composed of layered V_2VI_3 nanoplates and a nonconductive polymer. In this work, highly flexible and free-standing thermoelectric fabrics based on layered Bi_2Se_3 nanoplate/PVDF composites was fabricated with a simple peel-off method. The fabricated thermoelectric fabrics show a high room temperature power factor of $\sim 30\ \mu W\ m^{-1}K^{-2}$, low thermal conductivity of $0.42\ W\ K^{-1}\ m^{-1}$, and a resulting ZT value of ~0.02. Temperature-dependent thermoelectric properties and durability of the fabrics were measured. We anticipate that this work could pave the way for fabricating high performance flexible thermoelectric generators.

2. EXPERIMENTAL SECTION

Fabrication of Bi_2Se_3 Nanoplates and Composites. To fabricate the Bi_2Se_3 nanoplates, 1 mmol $Bi(NO_3)_3$ and 1.5 mmol Na_2SeO_3 were dissolved in 35 mL ethylene glycol with vigorous stirring followed by refluxing the mixture solution at 240 °C for 5 h. After the mixture cooled to room temperature, isopropyl alcohol was used to precipitate the fabricated Bi_2Se_3 nanoplates, which were then redissolved by acetone. This process was repeated three times to remove any unreacted chemicals and ethylene glycol from the surface. After drying, 270 mg layered Bi_2Se_3 nanoplates and 135 mg PVDF (2:1 ratio) were dissolved in 5 mL dimethylformamide (DMF) and sonicated for 3 h to ensure mixture uniformity. The solution was then drop-cast on glass substrates and baked on a hot plate at 80 °C overnight in air.

Characterization. The synthesized Bi_2Se_3 nanoplates were analyzed by X-ray diffraction (XRD) using Cu Kα radiation (Bruker D2 Phaser). The morphology and energy dispersive spectrometry (EDS) were measured by a scanning electron microscope (SEM, JEOL, JSM-6330F). Transmission electron microscope (TEM) techniques, including selected area electron diffraction (SAED) images, were performed using a JEM-2100 electron microscope. Raman measurements were performed on a Horiba−Jobin−Yvon Lab Raman HR confocal microscope using the 488 nm excitation line at room temperature.

Thermoelectric Properties. The thermoelectric properties of the Bi_2Se_3 nanoplate/PVDF composites were measured using a custom built apparatus similar to that reported by Kim et al.[27] A typical 4-probe technique was used to measure the electrical conductivity. The standard correction term was introduced here due to the finite dimensions of the probes and boundaries of the sample.[28] The Seebeck coefficient was measured by heating one copper block and simultaneously measuring the generated ΔT and thermoelectric voltage. A schematic and description of the measurement setup is included in the Supporting Information. This system was calibrated using a standard constantan sample, including subtraction of the contribution from gold plated voltage probes. The thermal conductivity was calculated using the relationship $\kappa = DC_p\rho$, where ρ, D, and C_p are the density, thermal diffusivity, and specific heat, respectively, which were measured by the laser flash diffusivity apparatus (Netzsch LFA 457) under an argon atmosphere. The size of the samples to measure the thermal conductivity is approximately 6 mm × 10 mm × 300 μm in width, length, and thickness, respectively. Here, because the Bi_2Se_3 nanoplates are randomly dispersed in the PVDF matrix, only thermal conductivity in the cross-plane was measured. Three samples were used, and each sample was tested at least 3 times from different points to ensure the reproducibility of the results. The average thermal diffusivity, density, and specific heat are $0.118\ mm^2\ s^{-1}$, $3.97\ g\ cm^{-3}$, and $0.897\ J\ g^{-1}\ K^{-1}$, respectively.

RESULTS AND DISCUSSION

Figure 1(a) shows a representative SEM image of the layered Bi_2Se_3 nanoplates, which demonstrate a hexagonal structure with an average planar dimension of ~1 μm. The contours of the overlap between two nanoplates in the image could be clearly distinguished. Following previously reported studies,[29] these nanoplates should be several QLs. Figure 1(b) and (c) show the TEM images of the Bi_2Se_3 nanoplates, which reveal the single crytal structure of the nanoplates. Figure 1(c) is a high resolution TEM image acquired along the [001] crystal direction of a Bi_2Se_3 nanoplate, and the inset shows the corresponding properly indexed selected area electron diffraction (SAED) pattern. Raman spectra of the layered and bulk Bi_2Se_3 were compared as shown in Figure 1(d). The three Raman peaks centered at approximately 70, 130, and 173 cm^{-1} could be assigned to the out-plane (A^1_{1g}), in-plane (E^2_g), and out-plane vibrational mode (A^2_{1g}) of Bi_2Se_3, respectively.[24] The relative intensity of the A^1_{1g} vibrational mode in the layered Bi_2Se_3 spectrum is stronger than that in the bulk Bi_2Se_3 spectrum. These Raman results confirm the few-layer structure of Bi_2Se_3. Furthermore, XRD measurements of the Bi_2Se_3 nanoplates were performed (see Figure 1(e)). The diffraction peaks are in good agreement with those of standard Bi_2Se_3 (JCPDS No. 89-2008). Additionally, EDS confirmed the existence of Bi and Se elements with an approximate atomic ratio of 2:3 in the fabircated sample, as shown in Figure 1(f).

Figure 2(a) illustrates the fabrication process of free-standing thermoelectric fabrics based on layered Bi_2Se_3 nanoplate/PVDF composites. Briefly, the desired amount of layered Bi_2Se_3 nanoplates and PVDF were ultrasonically dispersed in DMF solution. The resulting dispersion was directly drop-cast on a glass substrate followed by overnight annealing at 80 °C in air atmosphere (Figure 2(a), left image). After drying the solvent, free-standing fabrics based on layered Bi_2Se_3 nanoplate/PVDF composites were peeled off of the glass substrate (Figure 2(a), right image). Figure 2(b) shows an SEM image of a curved fabric. Figure 2(c) shows the cross section of the thermoelectric fabrics with a calculated thickness of ~12 μm. It is found that the layered Bi_2Se_3 nanoplates remained unchanged with plenty of grain boundaries that might result in reduced thermal conductivity of the composites. Photographs of the thermoelectric fabric are shown in Figure 2(d), which illustrates its high flexibility.

DOI: 10.1021/acsami.5b00514
ACS Appl. Mater. Interfaces 2015, 7, 7054−7059

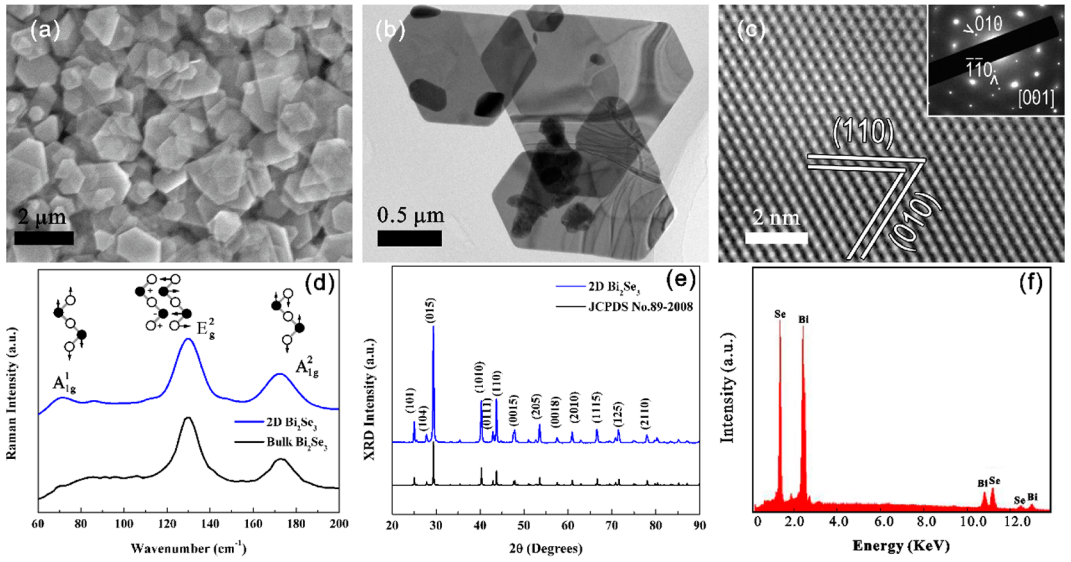

Figure 1. (a) SEM image, (b) TEM image, (c) high-resolution TEM image (inset shows the SAED pattern), (d) Raman spectra, (e) XRD spectrum, and (f) EDS of the Bi_2Se_3 nanoplates.

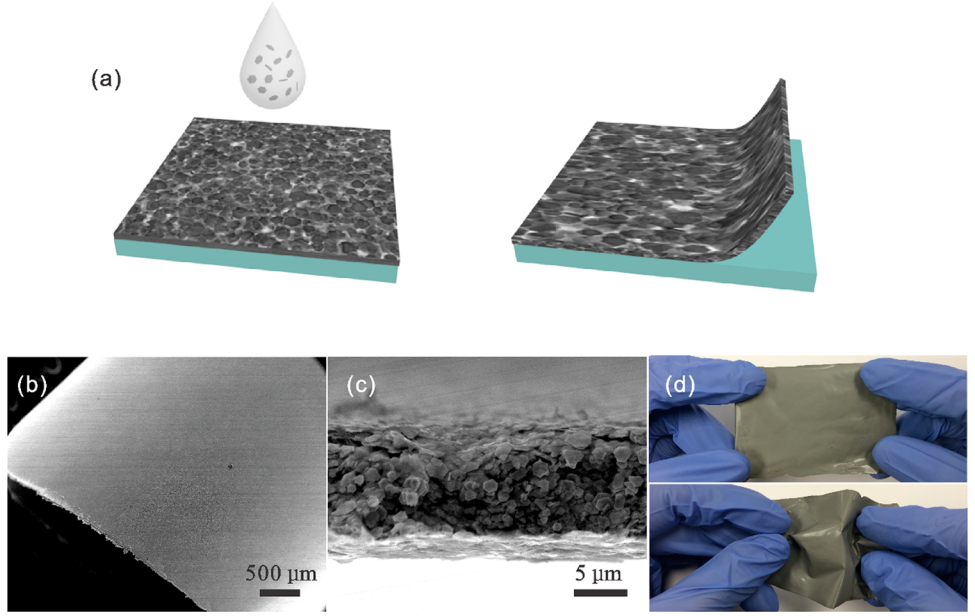

Figure 2. (a) Schematic diagram of the fabrication process of layered Bi_2Se_3 nanoplate/PVDF composite-based thermoelectric fabrics. (b) SEM image of a curved themoelectric fabric. (c) Cross-section of the Bi_2Se_3 nanoplate-based thermoelectric fabric. (d) Photographs of the flexible thermoelectric fabric, which show its high flexibility.

The temperature-dependent electrical conductivity for the Bi_2Se_3 nanoplate/PVDF composites is shown in Figure 3(a). The room temperature value of 5100 S m^{-1} is about one-third that reported for a single Bi_2Se_3 layer (see Table 1), but lower conductivity is to be expected. It is known that the electical conductivity depends significantly on the structures, the size of the nanoplates, and so forth. Therefore, the reduction in electical conductivity here is caused by scattering of carriers by the polymer within the nanoplate−nanoplate junctions. Despite the reduced conductivity by incorporation of nanoplates in the composite, the temperature-dependent conductivity exhibits metallic behavior exemplified by the negative slope with respect to temperature. The metallic conduction could be seen in high carrier-concentration small band gap semiconductors.[30] Metallic electrical conductivity is typically described by the Bloch−Grüneisen model, which is characterized by a near linear negative slope and low temperature leveling of conductivity due to a defect in the scattering residual resistivity, which is in accordance with the data shown in Figure 3(a).

The temperature dependence of the Seebeck coefficient for the nanoplate/polymer composites is shown in Figure 3(c). The room temperature value of −80 μV K^{-1} indicates a majority of electron carriers and is slightly less than the single layer value measured previously (see Table 1). This reduction is due to the fact that the total Seebeck coefficient is determined by a thermal conductivity weighted contribution from each component in the composite. Because ΔT is measured across the entire composite, but only the Bi_2Se_3 nanoplates contribute to the thermoelctric voltage, the net Seebeck coefficient of the composite is slightly lower than that of bulk Bi_2Se_3. Interestingly, despite the metallic-like temperature-dependent electrical conductivity

DOI: 10.1021/acsami.5b00514
ACS Appl. Mater. Interfaces 2015, 7, 7054−7059

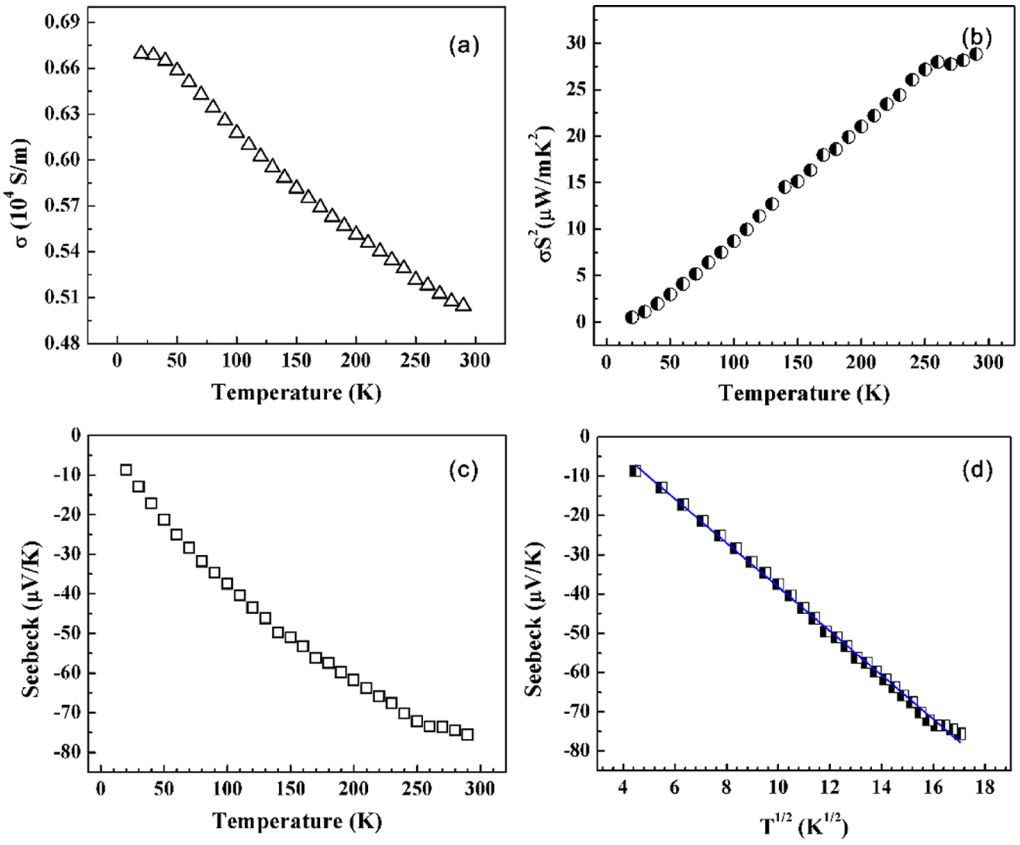

Figure 3. Temperature-dependent (a) electrical conductivity and (b) power factor of the thermoelectric fabrics. (c) Plot of Seebeck coefficient of the thermoelectric fabrics versus temperature in a linear scale. (d) Plot of Seebeck coefficient versus $T^{1/2}$.

Table 1. Comparison of Room Temperature (~300 K) Performance of Reported Bi_2Se_3-Based Thermoelectrics and the Layered Bi_2Se_3 Nanoplate/PVDF Composite-Based Thermoelectric Fabrics in This Work[a]

	σ (10^4 S m^{-1})	α (μV K^{-1})	power factor (μW m^{-1}K^{-2})	κ (W K^{-1} m^{-1})	ZT[b]	ref
bulk Bi_2Se_3	1.2	−83	82.7	1.1	0.02	16
Bi_2Se_3 single layer	1.8	−90	145.8	0.42	0.10	16
Bi_2Se_3 nanoplatelet-based composite pellets	4.3	−80	275.2	0.75	0.11	17
Bi_2Se_3 nanoplate/PVDF composite	0.51	−80	32.6	0.42	0.02	this work

[a]Some parameters in the reference work are estimated from graphs. [b]At room temperature.

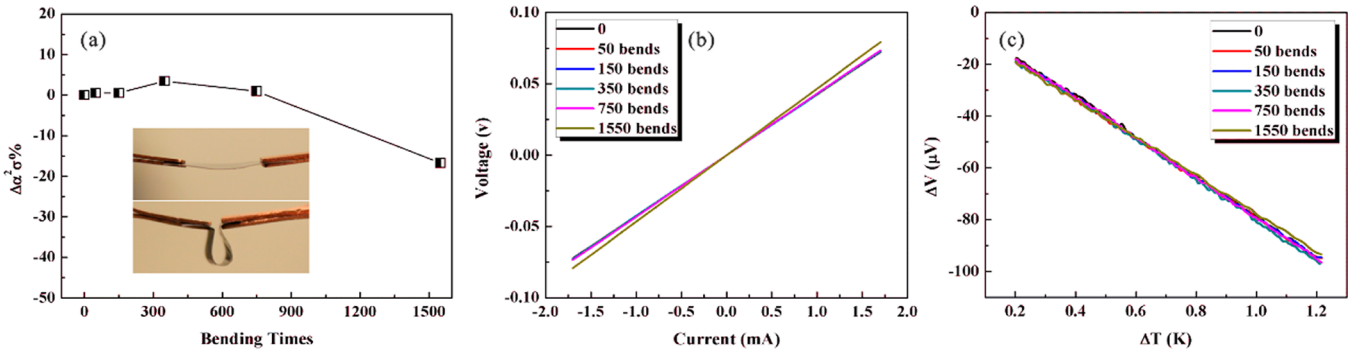

Figure 4. (a) Reliability of a layered Bi_2Se_3 nanoplate/PVDF composite with the inset image demonstrating a bending test. (b) Voltage−current and (c) $\Delta V-\Delta T$ lines representing the conductivity and Seebeck coefficient, respectively, at different numbers of bends.

behavior, the temperature-dependent Seebeck coefficient does not indicate complete metallic-like behavior. Typically, metallic thermoelectric behavior exhibits a linear temperature dependence, but the Bi_2Se_3 nanoplate/PVDF composites exhibit a slightly decreasing slope with increasing temperature. This behavior is typically described by a heterogeneous model characterized by a linear metallic term plus a modified $T^{1/2}$ exponentially weighted semiconducting term, which arises from nanoplate−nanoplate junctions.[31−33] The model is given by

$$\alpha(T) = aT + cT^{1/2}\exp\left[-\left(\frac{T_1}{T}\right)^{1/1+d}\right]$$

DOI: 10.1021/acsami.5b00514
ACS Appl. Mater. Interfaces 2015, 7, 7054−7059

where a and c are constants governing the linear and $T^{1/2}$ contributions, respectively, T_1 is an energy barrier constant for hopping from nanoplate to nanoplate, and d is the dimensionality of the conducting material. In this case, a dimensionality of 2 demonstrates the low space-filling percolation network of the Bi_2Se_3 nanoplates. The resulting fitting curve is shown in Figure 3(d).

These electrical conductivity and Seebeck coefficient values combine to yield the power factor given by $\alpha^2\sigma$ as shown in Figure 3(b). Table 1 compares the room temperature thermoelectric performance between reported Bi_2Se_3-based thermoelectrics and the layered Bi_2Se_3 nanoplate/PVDF composite-based thermoelectric fabrics developed in this work. The thermal conductivity of the fabric at room temperature is 0.42 $W K^{-1} m^{-1}$, which is much lower than that of bulk Bi_2Se_3 and the Bi_2Se_3 nanoplatelet-based composite pellets. The low thermal conductivity should be attributed not only to the use of PVDF in the heterogeneous structure but also to the grain boundaries in the platelets (see Figure 2(c)). The resulting ZT value of the thermoelectric fabric is calculated as 0.02, which is close to that of bulk Bi_2Se_3. Figure 4 demonstrates the reliability of the thermoelectric properties of a Bi_2Se_3 nanoplate/PVDF composite after a bending test. The power factor only decreases by ~15% after 1500 bends, which is the result of slightly decreased electrical conductivity after many bends as shown in Figure 4 (b). The reliability of the 2D nanoplate-based thermoelectric fabrics is much better than that of nanorod-based thermoelectric fabrics.[34] Overall, this demonstrates the feasibility of using these Bi_2Se_3 nanoplate-based composites in kinetic applications.

3. CONCLUSION

The flexible thermoelectric fabrics based on the layered Bi_2Se_3 nanoplate/PVDF composites is a typical example showing the promise of applications for 2D V_2VI_3 compounds, including Bi_2Se_3, Bi_2Te_3, and Sb_2Te_3. The comparable Seebeck coefficient to the single layer value results in favorable voltage outputs, whereas the reduced electrical conductivity may eventually be increased by further optimization of the device. These composites could then have the potential to be used in flexible and lightweight personal and portable electronics in which waste heat is available.

■ ASSOCIATED CONTENT

Supporting Information

Experimental setup for thermoelectric measurements. This material is available free of charge via the Internet at http://pubs.acs.org.

■ AUTHOR INFORMATION

Corresponding Authors

*E-mail: huangh@wfu.edu.
*E-mail: carroldl@wfu.edu.

Notes

The authors declare no competing financial interest.

■ ACKNOWLEDGMENTS

This study was conducted under support from the Air Force Office of Scientific Research Grant FA 9550-13-1-0085.

■ REFERENCES

(1) Hewitt, C. A.; Kaiser, A. B.; Roth, S.; Craps, M.; Czerw, R.; Carroll, D. L. Multilayered Carbon Nanotube/Polymer Composite Based Thermoelectric Fabrics. *Nano Lett.* **2012**, *12* (3), 1307−1310.
(2) Fan, Z.; Razavi, H.; Do, J.-w.; Moriwaki, A.; Ergen, O.; Chueh, Y.-L.; Leu, P. W.; Ho, J. C.; Takahashi, T.; Reichertz, L. A.; Neale, S.; Yu, K.; Wu, M.; Ager, J. W.; Javey, A. Three-dimensional nanopillar-array photovoltaics on low-cost and flexible substrates. *Nat. Mater.* **2009**, *8* (8), 648−653.
(3) Yoon, J.; Baca, A. J.; Park, S.-I.; Elvikis, P.; Geddes, J. B.; Li, L.; Kim, R. H.; Xiao, J.; Wang, S.; Kim, T.-H.; Motala, M. J.; Ahn, B. Y.; Duoss, E. B.; Lewis, J. A.; Nuzzo, R. G.; Ferreira, P. M.; Huang, Y.; Rockett, A.; Rogers, J. A. Ultrathin silicon solar microcells for semitransparent, mechanically flexible and microconcentrator module designs. *Nat. Mater.* **2008**, *7* (11), 907−915.
(4) Yang, R.; Qin, Y.; Dai, L.; Wang, Z. L. Power generation with laterally packaged piezoelectric fine wires. *Nat. Nanotechnol.* **2009**, *4* (1), 34−39.
(5) Kim, S. J.; We, J. H.; Cho, B. J. A wearable thermoelectric generator fabricated on a glass fabric. *Energy Environ. Sci.* **2014**, *7* (6), 1959−1965.
(6) Bubnova, O.; Khan, Z. U.; Malti, A.; Braun, S.; Fahlman, M.; Berggren, M.; Crispin, X. Optimization of the thermoelectric figure of merit in the conducting polymer poly(3,4-ethylenedioxythiophene). *Nat. Mater.* **2011**, *10* (6), 429−433.
(7) Chabinyc, M. Thermoelectric polymers: Behind organics' thermopower. *Nat. Mater.* **2014**, *13* (2), 119−121.
(8) Du, Y.; Shen, S. Z.; Cai, K.; Casey, P. S. Research progress on polymer−inorganic thermoelectric nanocomposite materials. *Prog. Polym. Sci.* **2012**, *37* (6), 820−841.
(9) Du, Y.; Cai, K. F.; Chen, S.; Cizek, P.; Lin, T. Facile Preparation and Thermoelectric Properties of Bi_2Te_3 Based Alloy Nanosheet/PEDOT:PSS Composite Films. *ACS Appl. Mater. Interfaces* **2014**, *6* (8), 5735−5743.
(10) Kim, G. H.; Shao, L.; Zhang, K.; Pipe, K. P. Engineered doping of organic semiconductors for enhanced thermoelectric efficiency. *Nat. Mater.* **2013**, *12* (8), 719−723.
(11) Kim, D.; Kim, Y.; Choi, K.; Grunlan, J. C.; Yu, C. Improved Thermoelectric Behavior of Nanotube-Filled Polymer Composites with Poly(3,4-ethylenedioxythiophene) Poly(styrenesulfonate). *ACS Nano* **2010**, *4* (1), 513−523.
(12) Yao, Q.; Chen, L.; Zhang, W.; Liufu, S.; Chen, X. Enhanced Thermoelectric Performance of Single-Walled Carbon Nanotubes/Polyaniline Hybrid Nanocomposites. *ACS Nano* **2010**, *4* (4), 2445−2451.
(13) Yao, Q.; Wang, Q.; Wang, L.; Chen, L. Abnormally enhanced thermoelectric transport properties of SWNT/PANI hybrid films by the strengthened PANI molecular ordering. *Energy Environ. Sci.* **2014**, *7*, 3801−3807.
(14) He, M.; Ge, J.; Lin, Z.; Feng, X.; Wang, X.; Lu, H.; Yang, Y.; Qiu, F. Thermopower enhancement in conducting polymer nanocomposites via carrier energy scattering at the organic-inorganic semiconductor interface. *Energy Environ. Sci.* **2012**, *5* (8), 8351−8358.
(15) Hewitt, C. A.; Kaiser, A. B.; Roth, S.; Craps, M.; Czerw, R.; Carroll, D. L. Varying the concentration of single walled carbon nanotubes in thin film polymer composites, and its effect on thermoelectric power. *Appl. Phys. Lett.* **2011**, *98* (18), 183110.
(16) Sun, Y.; Cheng, H.; Gao, S.; Liu, Q.; Sun, Z.; Xiao, C.; Wu, C.; Wei, S.; Xie, Y. Atomically Thick Bismuth Selenide Freestanding Single Layers Achieving Enhanced Thermoelectric Energy Harvesting. *J. Am. Chem. Soc.* **2012**, *134* (50), 20294−20297.
(17) Soni, A.; Yanyuan, Z.; Ligen, Y.; Aik, M. K. K.; Dresselhaus, M. S.; Xiong, Q. Enhanced Thermoelectric Properties of Solution Grown $Bi_2Te_{3-x}Se_x$ Nanoplatelet Composites. *Nano Lett.* **2012**, *12* (3), 1203−1209.
(18) Goyal, V.; Teweldebrhan, D.; Balandin, A. A. Mechanically-exfoliated stacks of thin films of Bi_2Te_3 topological insulators with enhanced thermoelectric performance. *Appl. Phys. Lett.* **2010**, *97* (13), 133117.

DOI: 10.1021/acsami.5b00514
ACS Appl. Mater. Interfaces 2015, 7, 7054−7059

(19) Zahid, F.; Lake, R. Thermoelectric properties of Bi_2Te_3 atomic quintuple thin films. *Appl. Phys. Lett.* **2010**, *97* (21), 212102.
(20) Son, J. S.; Choi, M. K.; Han, M.-K.; Park, K.; Kim, J.-Y.; Lim, S. J.; Oh, M.; Kuk, Y.; Park, C.; Kim, S.-J.; Hyeon, T. n-Type Nanostructured Thermoelectric Materials Prepared from Chemically Synthesized Ultrathin Bi_2Te_3 Nanoplates. *Nano Lett.* **2012**, *12* (2), 640−647.
(21) Poudel, B.; Hao, Q.; Ma, Y.; Lan, Y.; Minnich, A.; Yu, B.; Yan, X.; Wang, D.; Muto, A.; Vashaee, D.; Chen, X.; Liu, J.; Dresselhaus, M. S.; Chen, G.; Ren, Z. High-Thermoelectric Performance of Nanostructured Bismuth Antimony Telluride Bulk Alloys. *Science* **2008**, *320* (5876), 634−638.
(22) Xia, Y.; Qian, D.; Hsieh, D.; Wray, L.; Pal, A.; Lin, H.; Bansil, A.; Grauer, D.; Hor, Y. S.; Cava, R. J.; Hasan, M. Z. Observation of a large-gap topological-insulator class with a single Dirac cone on the surface. *Nat. Phys.* **2009**, *5* (6), 398−402.
(23) Zhang, H.; Liu, C.-X.; Qi, X.-L.; Dai, X.; Fang, Z.; Zhang, S.-C. Topological insulators in Bi_2Se_3, Bi_2Te_3 and Sb_2Te_3 with a single Dirac cone on the surface. *Nat. Phys.* **2009**, *5* (6), 438−442.
(24) Huang, H.; Li, Y.; Li, Q.; Li, B.; Song, Z.; Huang, W.; Zhao, C.; Zhang, H.; Wen, S.; Carroll, D.; Fang, G. Field electron emission of layered Bi_2Se_3 nanosheets with atom-thick sharp edges. *Nanoscale* **2014**, *6* (14), 8306−8310.
(25) Tretiakov, O. A.; Abanov, A.; Murakami, S.; Sinova, J. Large thermoelectric figure of merit for three-dimensional topological Anderson insulators via line dislocation engineering. *Appl. Phys. Lett.* **2010**, *97* (7), 073108.
(26) Ghaemi, P.; Mong, R. S. K.; Moore, J. E. In-Plane Transport and Enhanced Thermoelectric Performance in Thin Films of the Topological Insulators. *Phys. Rev. Lett.* **2010**, *105* (16), 166603.
(27) Kim, G. T.; Park, J. G.; Lee, J. Y.; Yu, H. Y.; Choi, E. S.; Suh, D. S.; Ha, Y. S.; Park, Y. W. Simple technique for the simultaneous measurements of the four-probe resistivity and the thermoelectric power. *Rev. Sci. Instrum.* **1998**, *69* (10), 3705−3706.
(28) Zimney, E. J.; Dommett, G. H. B.; Ruoff, R. S.; Dikin, D. A. Correction factors for 4-probe electrical measurements with finite size electrodes and material anisotropy: a finite element study. *Meas. Sci. Technol.* **2007**, *18*, 2067−2073.
(29) Zhang, J.; Peng, Z.; Soni, A.; Zhao, Y.; Xiong, Y.; Peng, B.; Wang, J.; Dresselhaus, M. S.; Xiong, Q. Raman Spectroscopy of Few-Quintuple Layer Topological Insulator Bi_2Se_3 Nanoplatelets. *Nano Lett.* **2011**, *11* (6), 2407−2414.
(30) Hor, Y. S.; Richardella, A.; Roushan, P.; Xia, Y.; Checkelsky, J. G.; Yazdani, A.; Hasan, M. Z.; Ong, N. P.; Cava, R. J. P-type Bi_2Se_3 for topological insulator and low-temperature thermoelectric applications. *Phys. Rev. B* **2009**, *79* (19), 195208.
(31) Choi, Y.-M.; Lee, D.-S.; Czerw, R.; Chiu, P.-W.; Grobert, N.; Terrones, M.; Reyes-Reyes, M.; Terrones, H.; Charlier, J.-C.; Ajayan, P. M.; Roth, S.; Carroll, D. L.; Park, Y.-W. Nonlinear Behavior in the Thermopower of Doped Carbon Nanotubes Due to Strong, Localized States. *Nano Lett.* **2003**, *3* (6), 839−842.
(32) Kaiser, A. B.; Düsberg, G.; Roth, S. Heterogeneous model for conduction in carbon nanotubes. *Phys. Rev. B* **1998**, *57* (3), 1418−1421.
(33) Carroll, D. L.; Czerw, R.; Webster, S. Polymer−nanotube composites for transparent, conducting thin films. *Synth. Met.* **2005**, *155*, 694−697.
(34) Dun, C.; Hewitt, C.; Huang, H.; Montgomery, D.; Xu, J.; Carroll, D. Flexible Thermoelectric Fabrics Based on Self-assembled Tellurium Nanorods with a Large Power Factor. *Phys. Chem. Chem. Phys.* **2015**, DOI: 10.1039/C4CP05390G.

DOI: 10.1021/acsami.5b00514
ACS Appl. Mater. Interfaces 2015, 7, 7054−7059